5.6. Barrow, Alaska (01/14/11 – 11/28/11)

This section describes quality control of solar data recorded at Barrow between 01/14/11 – 11/28/11. No site visit was performed during this period. A total of 10,003 SUV scans are part of the Barrow Volume 21 dataset.

Data collected during the reporting period are affected by the following problem:

- Reduced duty cycle
  Like in previous years, the instrument's shutter became "sticky" at the end of the winter and there was the risk that it would not fully open during solar scans. The system's duty cycle was therefore reduced from four to two scans per hour from 3/29/11 onward.

5.6.1. Irradiance Calibration

The site irradiance standards of the reporting period were the lamps M-699, 200W009, and 200W042.

Lamp 200W042 was calibrated in June 2007 at BSI with four 1000-Watt FEL lamps provided by the Central UV Calibration Facility (CUCF) at Boulder. This calibration procedure was complicated by the fact that the irradiance scale of the four FEL lamps refers to the detector-based scale of the National Institute of Standards and Technology established in 2000 (NIST2000; Yoon et al., 2002), whereas all solar data of the NSF UVSIMN refer to the source-based NIST scale from 1990 (NIST1990, Walker et al., 1987). The NIST2000 scale is about 1.3% larger than the NIST1990 scale. Data of certificates issued by CUCF were converted to the NIST1990 scale before the calibration was transferred to the site standard.

Lamps M-699 and 200W009 were originally calibrated by Optronic Laboratories (OL) in March 2001. Both lamps were brought to San Diego in 2007 and recalibrated against lamps 200W028 and 200W022. (Lamp 200W028 is the San Diego site standard; lamp 200W022 is BSI's long-term standard, which preserves the OL scale from March 2001.)

The three lamps were compared to the traveling standard 200W017 in March 2010. The calibration of lamp 200W017 is traceable to the NIST1990 scale in the same way as lamp 200W042. At this time, the calibrations of the lamps agreed with that of 200W017 to within ±1.5%.

The three site standards were compared with each other on 7/4/11 (Figure 5.6.1) and 11/7/11 (Figure 5.6.2). Measurements agreed to within ±1.5% on both occasions, giving confidence in the stability of the lamps.

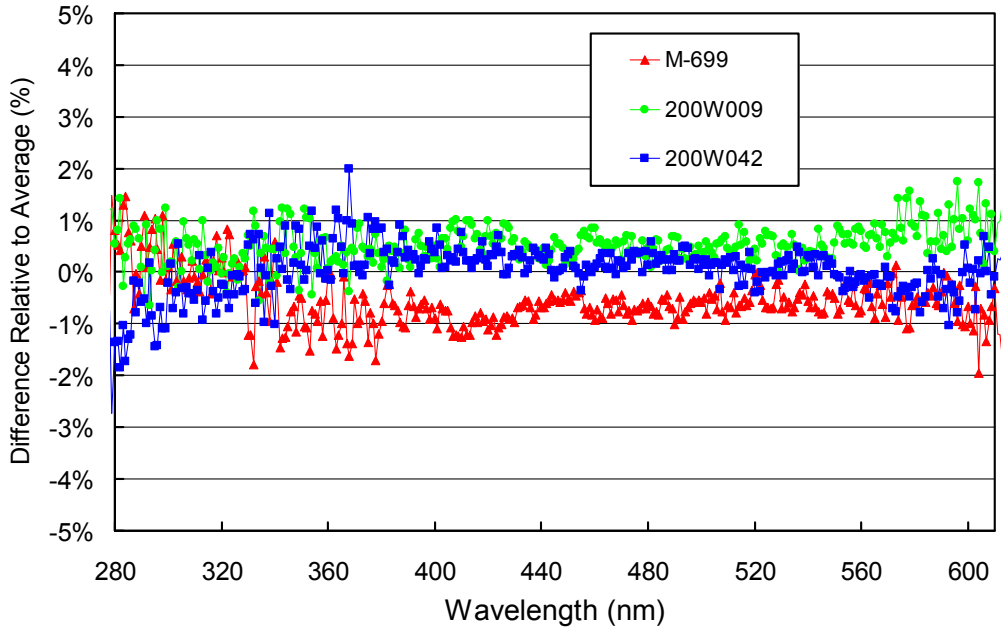

Figure 5.6.1. *Comparison of on-site lamps M-699, 200W009, and 200W042 with each other on 7/4/11.*

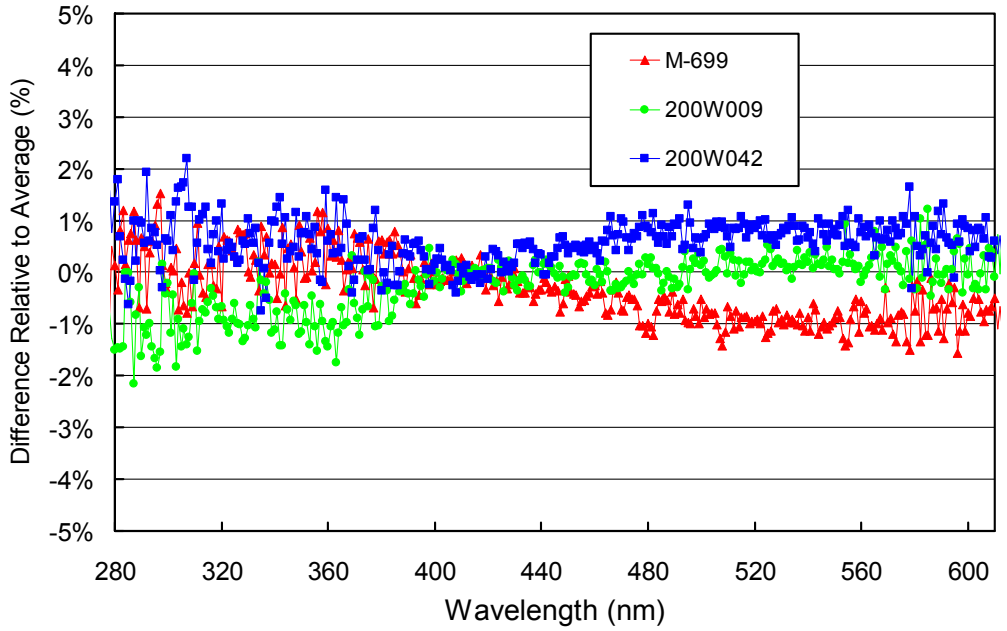

Figure 5.6.2. *Comparison of on-site lamps M-699, 200W009, and 200W042 with each other on 11/7/11.*

5.6.2. Instrument Stability and Calibration

The radiometric stability of the SUV-100 spectroradiometer was monitored with calibrations utilizing site irradiance standards, daily response scans of the internal irradiance reference lamp, and by comparison with the GUV-511 multifilter radiometer. The stability of this lamp is monitored with the TSI sensor, which is independent from possible monochromator and PMT drifts. By logging the PMT currents at several wavelengths during response scans, changes in monochromator throughput and PMT sensitivity can be detected.

Figure 5.6.3 shows changes in TSI readings and PMT currents at 300 and 400 nm, derived from the daily response scans of 2011. TSI measurements indicate that the internal lamp became darker by about 3% over time. PMT currents are tracking the TSI measurement very well, indicating excellent stability of monochromator throughput and PMT sensitivity. Two outliers occurred and are related to power outages resulting in the system temperature being out of range.

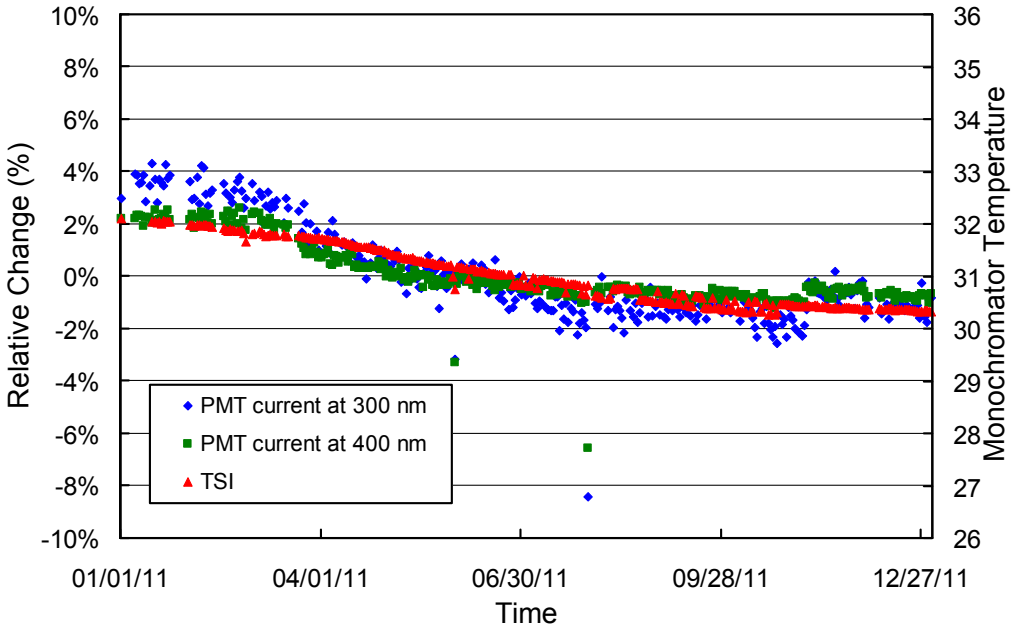

Figure 5.6.3. *Time-series of PMT current at 300 and 400 nm, and TSI signal extracted from measurements of the internal irradiance standard at Barrow. All data sets are normalized to their average.*

To adjust for the small change in responsivity, the reporting period was subdivided into three periods. Figure 5.6.4 shows the ratio of the irradiance assigned to the internal reference lamp in Period 1B (10/10/11 – 10/18/11) and P2 (10/19/11 – 12/31/11) relative to the spectral irradiance of Period P1 (01/01/11 – 10/09/11). The change in responsivity over the year is less than 3% at wavelengths. Note that the irradiance spectrum applied in Period P1B is the average of the spectra of Periods P1 and P2.

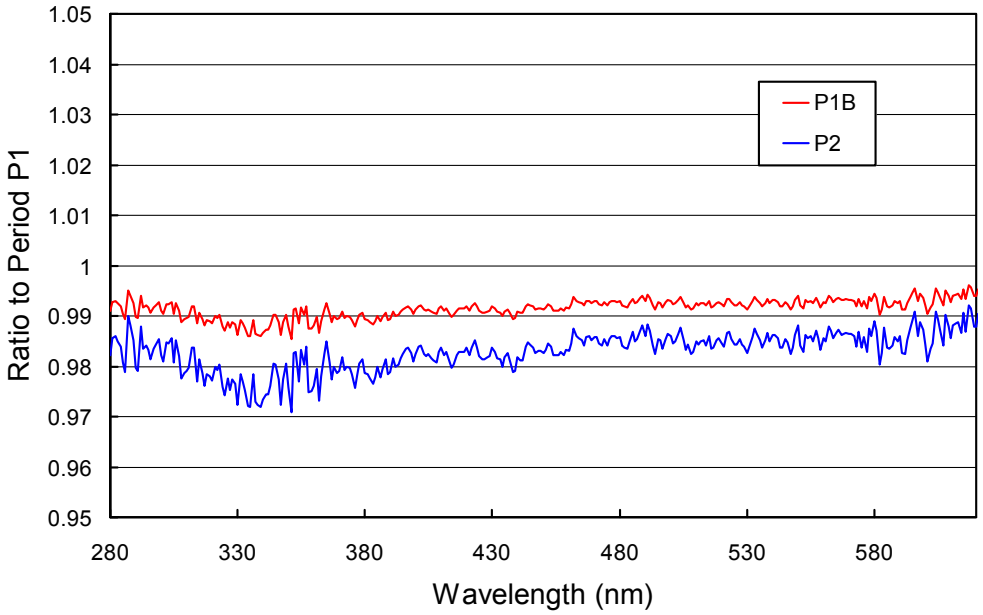

Figure 5.6.4. *Ratios of spectral irradiance assigned to the internal reference lamp during the Periods P1B and P2 relative to Period P1.*

Figure 5.6.5 presents ratios of standard deviation and average spectra, calculated from individual absolute scans performed in Periods 1 and 2. These ratios are useful for estimating the variability of calibrations assigned to each period. The variability is less than 1.5% for both periods.

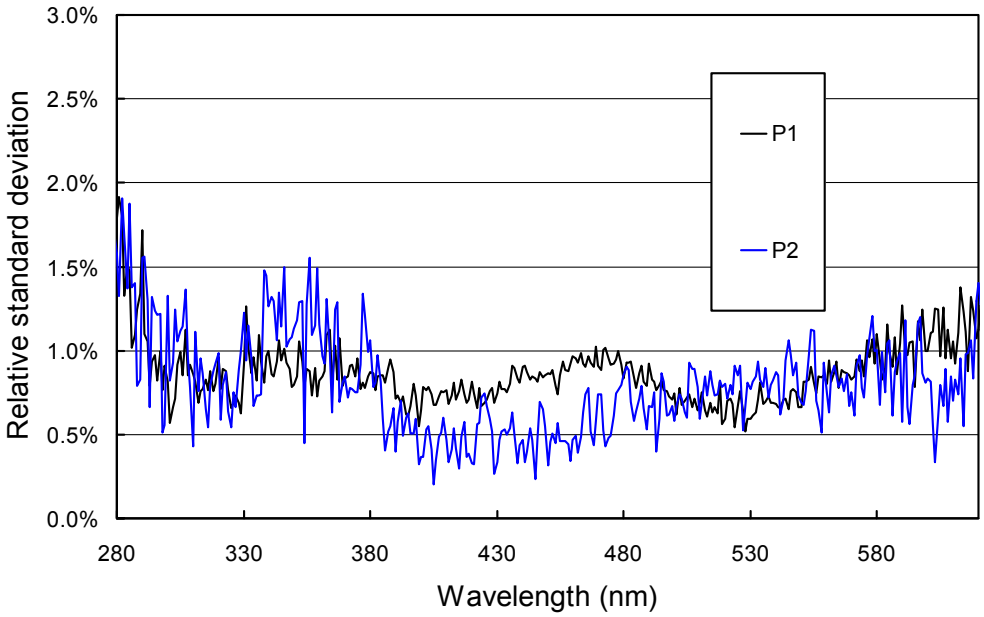

Figure 5.6.5. *Ratio of standard deviation and average spectra calculated from irradiance spectra applied to the internal lamp.*

All SUV-100 data were also compared to measurements of the collocated GUV-511 radiometer. The ratio of final GUV and SUV data at 340 nm as a function of time is shown in Figure 5.6.6. The standard deviation of the ratio is 0.04. Variability is smaller in the spring because of less influence by clouds.

As a last check of data quality, SUV-100 measurements were compared with radiative transfer calculations. These calculations are part of Version 2 processing (www.biospherical.com/NSF/Version2/). The ratio of measured and modeled data was generally within the range observed in past years.

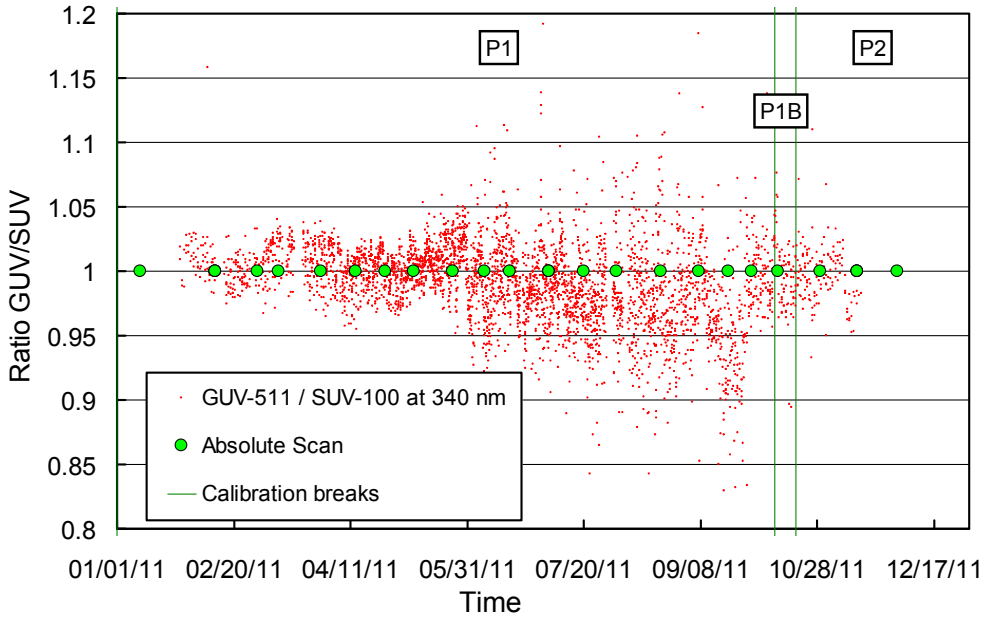

Figure 5.6.6. *Ratio of GUV-511 measurements of the 340-nm channel to SUV-100 measurements. The latter were weighted with the spectral response function of the 340-nm GUV-511 channel. Times of absolute scans and calibration breaks are also indicated.*

5.6.3. Wavelength Calibration

Wavelength stability of the system was monitored with the internal mercury lamp. Information from the daily wavelength scans was used to homogenize the data set by correcting day-to-day fluctuations in the wavelength offset. Figure 5.6.7 shows the differences in the wavelength offset of the 296.73 nm mercury line between two consecutive wavelength scans. In total 382 pairs, measured between 1/1/11 and 12/31/11, were evaluated. In 94% (94%) of all cases, the change in offset was smaller than ±0.025 nm (±0.055 nm). Most larger changes in wavelength offset were related to power outages and similar events and corrected during data processing.

The function for correcting the non-linearity of the monochromator's wavelength drive is shown in Figure 5.6.8. The function was calculated with the Version 2 Fraunhofer line correlation method (*Bernhard et al.*, 2004). Data were corrected with these functions and again tested with the correlation method. Results for four wavelengths in the UV and one in the visible are shown in Figure 5.6.9. Residual shifts in the UV are typically smaller than ±0.05 nm, except on 3/21/11, when they were about 0.1 nm. Wavelength errors, including the shift on 3/21/11, have been further reduced in the Version 2 data set.

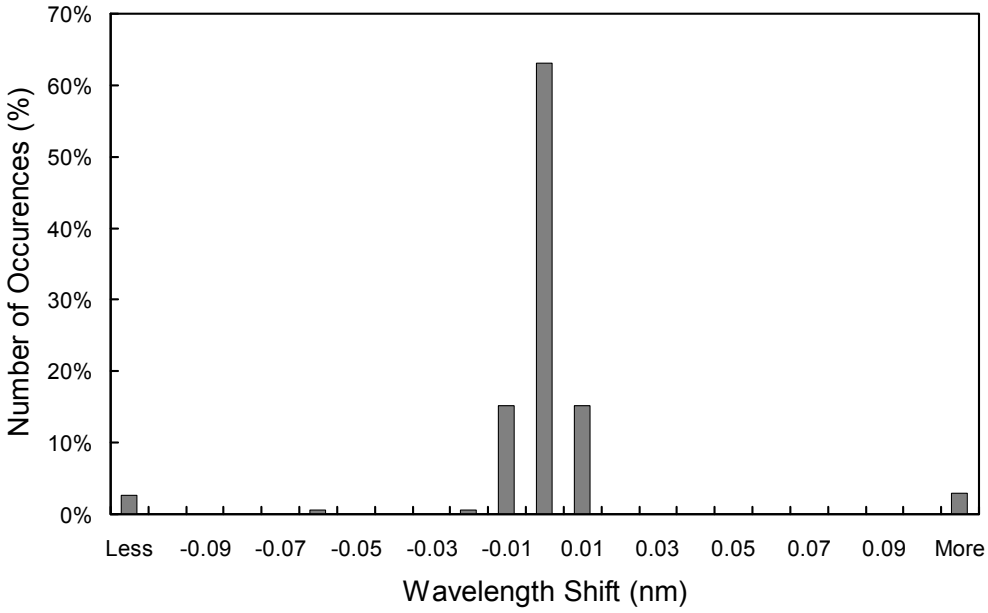

Figure 5.6.7. *Differences in the measured position of the 296.73 nm mercury line between consecutive wavelength scans. The x-labels give the center wavelength shift for each column. Thus the 0-nm histogram column covers the range -0.005 to +0.005 nm. "Less" means shifts smaller than –0.105 nm; "more" means shifts larger than 0.105 nm.*

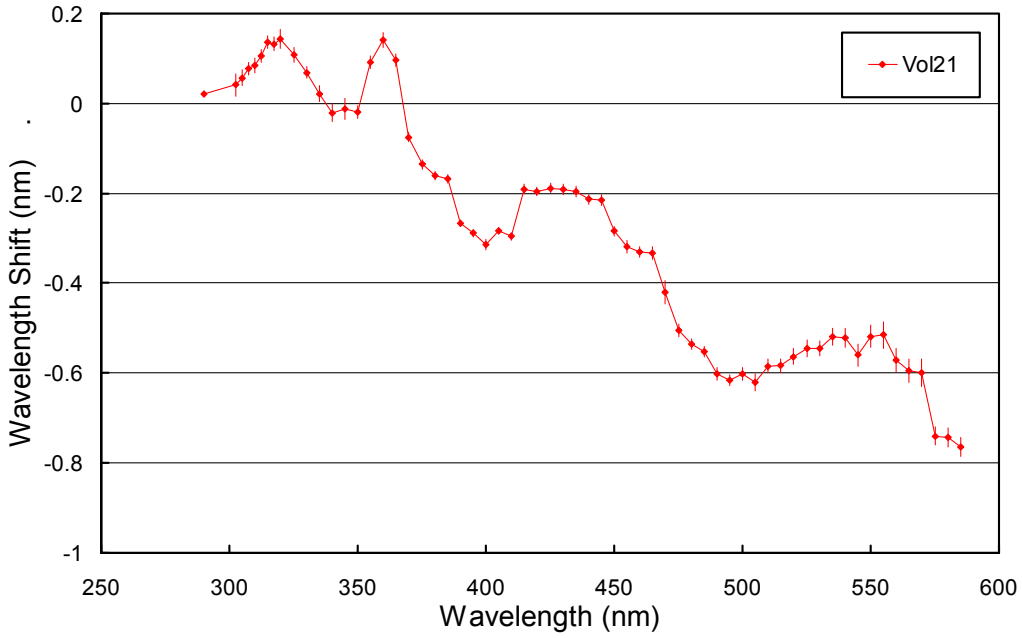

Figure 5.6.8. *Monochromator non-linearity correction functions for Barrow Volume 21. Error bars indicate the standard deviation of the data contributing to this plot.*

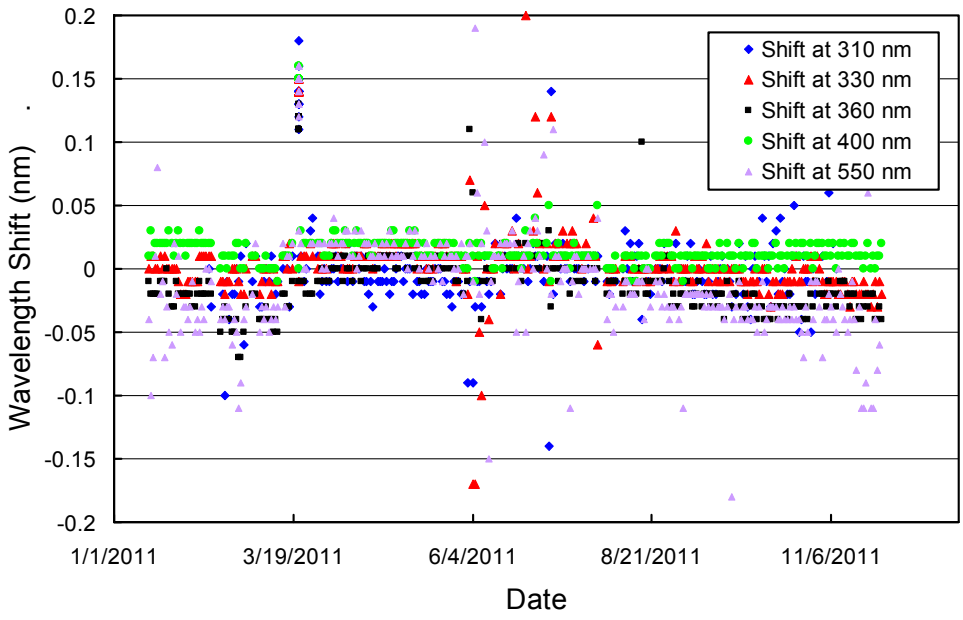

Figure 5.6.9. *Wavelength accuracy check of final data at four wavelengths in the UV and one in the visible by means of Fraunhofer-line correlation. The noontime measurement has been evaluated for each day of the reporting period when the Sun was above the horizon.*

5.6.4. Missing Data

A total of 10,003 scans are part of the Barrow Volume 21 dataset (01/14/11 – 11/28/11). There are no data for the following periods:

- 02/12/11 - 02/15/11: Monochromator wavelength lost due to operational error
- 02/27/11: System not running for unknown reasons
- 03/13/11: Computer powered off for unknown reasons wavelength position
- 03/19/11 - 03/20/11: Computer powered off for unknown reasons wavelength position
- 07/30/11 - 07/31/11: Power outage
- 08/06/11 - 08/07/11: Computer powered off for unknown reasons wavelength position
- 11/19/11: Data quality doubtful

5.6.5. GUV Data

The GUV-511 radiometer installed next to the SUV-100 was calibrated against final SUV-100 measurements following the procedure outlined in Section 4.3.1. Data products were calculated from calibrated measurements (Section 4.3.2). Figure 5.6.10. shows a comparison of GUV-511 and SUV-100 erythemal irradiance based on final Volume 21 data. For solar zenith angles smaller than 75°, measurements of the GUV-511 instrument are on average 4% larger than SUV-100 measurements. The bias between the two instruments depends somewhat on season. Some of the seasonality is caused by the simplifications of the GUV inversion procedure. Measurements of the GUV's 305 nm channel are close to the detection limit when SZA exceeds 75° and the total ozone column is large. The large noise in GUV data during those conditions also affects the calculation of secondary data products such as erythemal irradiance. We advise data users to use SUV-100 rather than GUV-511 data, in particular when the SZA exceeds 75°.

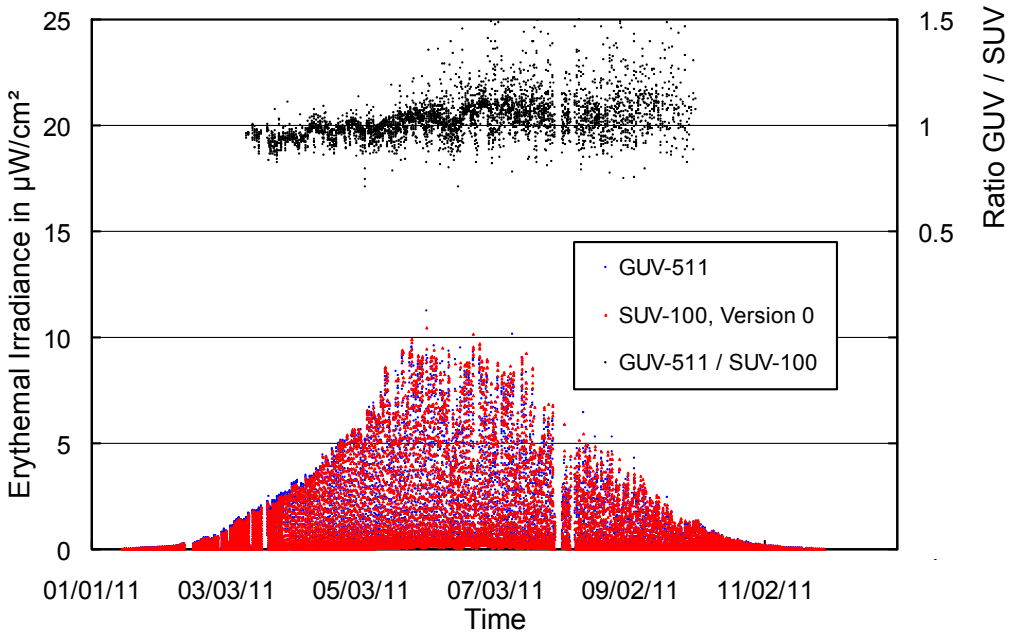

Figure 5.6.10. *Comparison of erythemal irradiance measured by the SUV-100 spectroradiometer and the GUV-511 radiometer. Data are based on "Version 0" (cosine-error uncorrected) data.*

Figure 5.6.11 shows a comparison of total ozone measurements from the GUV-511, the Ozone Monitoring Instrument (OMI) on NASA's AURA satellite (Version 8.5, Collection 3), and the SUV-100 (Version 2 data using climatological profiles with temperature correction). GUV-511 ozone values were calculated as described in Section 4.3.3. GUV-511 data measured between April and September are on average 1.2% larger than OMI data. Between February and March 15, during periods when total ozone was exceptionally small in 2011 (see Chapter 7.6), GUV-511 measurements tend to be low by about 3%. For SZAs larger than 75°, GUV-511 ozone data become unreliable and should not be used. SUV-100 ozone data exceed OMI measurements on average by 3%. The bias is somewhat larger during the low-ozone period in March. This discrepancy is likely due to the use of climatological profiles of calculating total zone from SUV data, which do not take the unprecedented situation of 2011 into account. For more information on total ozone calculation from SUV-data at Barrow see *Bernhard et al.*, 2003. The effect of the vertical distribution of ozone has been further discussed by *Bernhard et al.*, 2005.

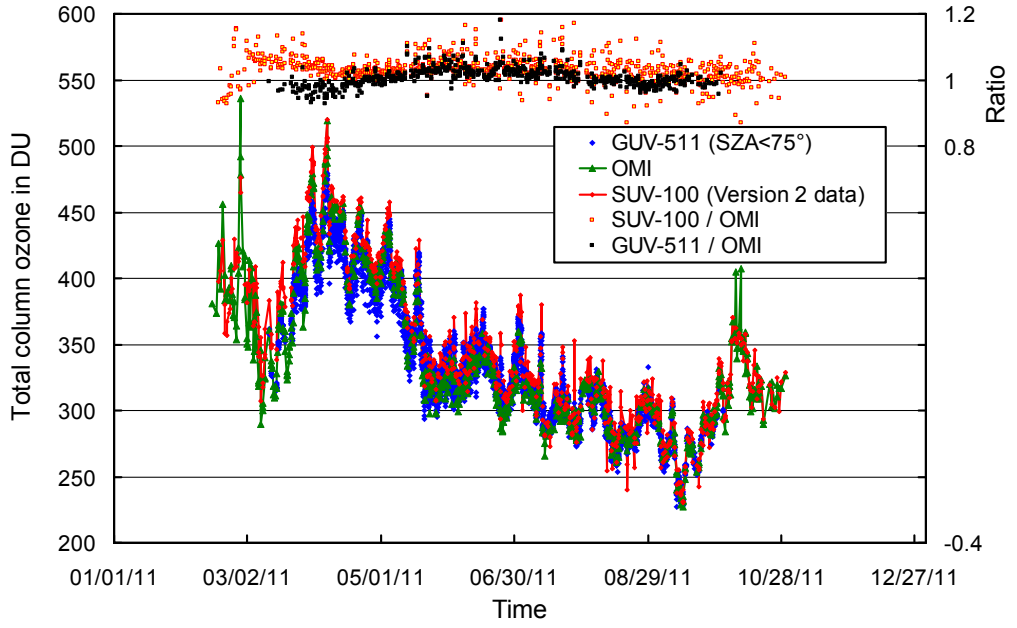

Figure 5.6.11. *Comparison of total column ozone measurements from GUV-511, OMI, and SUV-100. GUV-511 measurements are plotted in 30 minute intervals. For calculating the ratios of SUV-100/OMI and GUV-511/OMI, only measurements concurrent with the OMI overpass were evaluated.*

References

Bernhard, G., C.R. Booth, and R.D. McPeters. (2003). Calculation of total column ozone from global UV spectra at high latitudes. J. Geophys Research, 108(D17), 4532, doi:10.1029/2003JD003450.

Bernhard, G., C. R. Booth, and J. C. Ehramjian. (2004). Version 2 data of the National Science Foundation's Ultraviolet Radiation Monitoring Network: South Pole, J. Geophys. Res., 109, D21207, doi:10.1029/2004JD004937.

Bernhard, G., R.D. Evans, G.J. Labow, and S.J. Oltmans. (2005). Bias in Dobson Total Ozone Measurements at High Latitudes due to Approximations in Calculations of Ozone Absorption Coefficients and Airmass. J. Geophys. Res., 110, D10305, doi:10.1029/2004JD005559, 2005.